THE JOURNAL OF BIOLOGICAL CHEMISTRY VOL. 290, NO. 37, pp. 22747–22758, September 11, 2015

Neurotoxins from Snake Venoms and α-Conotoxin ImI Inhibit Functionally Active Ionotropic γ-Aminobutyric Acid (GABA) Receptors*

Received for publication, March 1, 2015, and in revised form, July 20, 2015 Published, JBC Papers in Press, July 28, 2015, DOI 10.1074/jbc.M115.648824

Denis S. Kudryavtsev[‡], Irina V. Shelukhina[‡], Lina V. Son[§1], Lucy O. Ojomoko[‡], Elena V. Kryukova[‡], Ekaterina N. Lyukmanova[‡‖2], Maxim N. Zhmak[‡¶], Dmitry A. Dolgikh[‡‖2], Igor A. Ivanov[‡], Igor E. Kasheverov[‡1], Vladislav G. Starkov[‡], Joachim Ramerstorfer[**], Werner Sieghart[**], Victor I. Tsetlin[‡], and Yuri N. Utkin[‡3]

From the [‡]Shemyakin-Ovchinnikov Institute of Bioorganic Chemistry, Russian Academy of Sciences, 16/10 Miklukho-Maklaya Street, Moscow 117997, Russia, the [§]Moscow Institute of Physics and Technology, Institutsky Per. 9, Dolgoprudny, Moscow Region 141700, Russia, the [¶]Syneuro OOO, ul. Miklukho-Maklaya 16/10, Moscow 117997, Russia, the [‖]Lomonosov Moscow State University, Moscow 119991, Russia, and the [**]Department of Molecular Neurosciences, Center for Brain Research, Medical University Vienna, A-1090 Vienna, Austria

Background: Different snake venom three-finger toxins interact with various receptors, channels, and membranes.
Results: Here, we demonstrate that $GABA_A$ receptors are inhibited by α-cobratoxin, other long chain α-neurotoxins, nonconventional toxin from *Naja kaouthia,* and α-conotoxin ImI.
Conclusion: Some toxin blockers of nicotinic acetylcholine receptors also inhibit $GABA_A$ receptors.
Significance: Three-finger toxins offer new scaffolds for the design of $GABA_A$ receptor effectors.

Ionotropic receptors of γ-aminobutyric acid ($GABA_AR$) regulate neuronal inhibition and are targeted by benzodiazepines and general anesthetics. We show that a fluorescent derivative of α-cobratoxin (α-Ctx), belonging to the family of three-finger toxins from snake venoms, specifically stained the α1β3γ2 receptor; and at 10 μM α-Ctx completely blocked GABA-induced currents in this receptor expressed in *Xenopus* oocytes (IC_{50} = 236 nM) and less potently inhibited α1β2γ2 ≈ α2β2γ2 > α5β2γ2 > α2β3γ2 and α1β3δ $GABA_A$Rs. The α1β3γ2 receptor was also inhibited by some other three-finger toxins, long α-neurotoxin Ls III and nonconventional toxin WTX. α-Conotoxin ImI displayed inhibitory activity as well. Electrophysiology experiments showed mixed competitive and noncompetitive α-Ctx action. Fluorescent α-Ctx, however, could be displaced by muscimol indicating that most of the α-Ctx-binding sites overlap with the orthosteric sites at the β/α subunit interface. Modeling and molecular dynamic studies indicated that α-Ctx or α-bungarotoxin seem to interact with $GABA_AR$ in a way similar to their interaction with the acetylcholine-binding protein or the ligand-binding domain of nicotinic receptors. This was supported by mutagenesis studies and experiments with α-conotoxin ImI and a chimeric *Naja oxiana* α-neurotoxin indicating that the major role in α-Ctx binding to $GABA_AR$ is played by the tip of its central loop II accommodating under loop C of the receptors.

Type A γ-aminobutyric acid receptor ($GABA_AR$)[4] is abundantly expressed across the nervous system. Most of the $GABA_A$Rs in the brain are constructed from α1–6 and β1–3 subunits co-assembled with γ1–3 or δ/ϵ/π/θ subunits. Interestingly, some β subunits, usually found in heteropentameric $GABA_A$Rs could also form constitutively active homopentameric ligand-gated ion channels. Channels with such properties were found in cultured neurons (1), and in fact the β3-homopentamer at the moment is the only $GABA_AR$ with known three-dimensional structure (2).

$GABA_A$Rs are targeted by diverse toxins of low molecular weight, such as the channel blocker picrotoxin (3), a polyacetylenic compound oenanthotoxin (4), the GABA site antagonist bicuculline (5), and by GABA site agonists such as ibotenic acid and muscimol. Benzodiazepines are positive allosteric modulators of $GABA_AR$ and were the world's most prescribed drugs in the 1980s (6). It is almost impossible to introduce fluorescent labels into such molecules, and therefore, they cannot be used in live cell imaging studies. In contrast, peptide toxins can easily be tagged with fluorescent or radioactive labels. Many of them, for example α-conotoxins from Conus snails and three-finger toxins (TFTs) from snake venoms, target nicotinic acetylcholine receptors (nAChRs) and show high levels of selectivity between the different nAChR types (7). For example, α-bungarotoxin (α-Bgt) from multibanded krait venom binds with nanomolar affinity to the muscle-type and α7 receptors but not to the heteropentameric neuronal nAChRs (8, 9). Such peptide toxins also could be quite helpful in structural studies. The x-ray crystal structure of the extracellular domain of α1 (10)

* This work was supported by Russian Science Foundation Grant 14-24-00118. The authors declare that they have no conflicts of interest with the contents of this article.
[1] Supported by Russian Foundation for Basic Research Grant 14-04-00885.
[2] Supported by Russian Science Foundation Grant 14-14-00255 (NT II/I chimeric toxin was obtained with this grant).
[3] To whom correspondence may be addressed: Shemyakin-Ovchinnikov Institute of Bioorganic Chemistry, Russian Academy of Sciences, Ul. Miklukho-Maklaya 16/10, Moscow V-437, 117997 Russia. Tel./Fax: 7-495-3366522; E-mail: utkin@mx.ibch.ru.

[4] The abbreviations used are: $GABA_AR$, type A γ-aminobutyric acid receptor; AChBP, acetylcholine-binding protein; α-Bgt, α-bungarotoxin; α-Ctx, α-cobratoxin; GlyR, glycine receptor; nAChR, nicotinic acetylcholine receptor; TFT, three-finger toxin; PDB, Protein Data Bank; NT II, neurotoxin II; Ls III, α-elapitoxin-Ls2a.

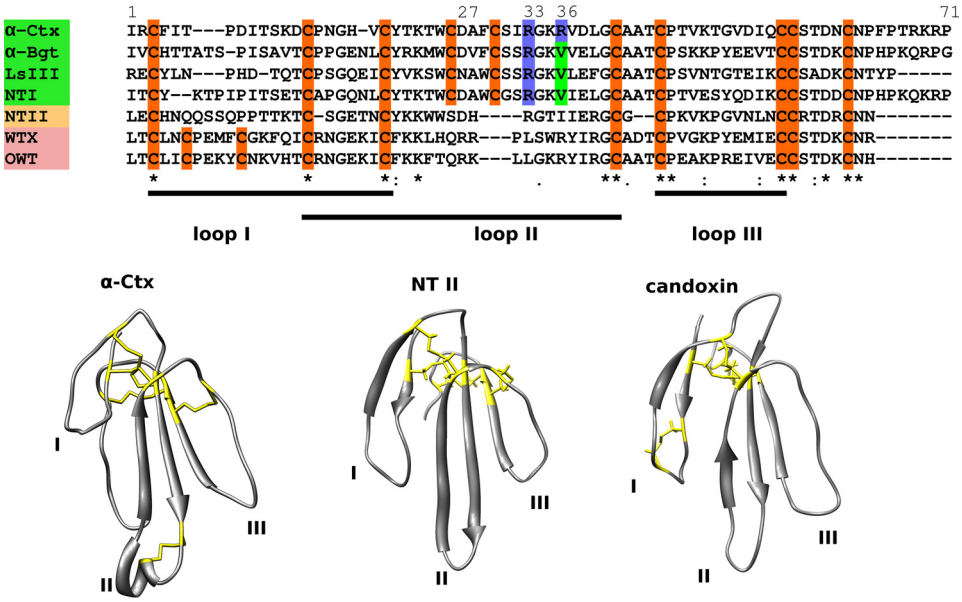

FIGURE 1. **Structural diversity of three-finger neurotoxins.** *Top set* represents sequence alignments. All TFTs have three loops stabilized by four disulfides, but some neurotoxins have one additional disulfide bond. Long (names higlighted *green*) and weak or nonconventional (names highlighted *pink*) neurotoxins have additional disulfide bonds in the second and the first loops, respectively, although short neurotoxins (name highlighted *yellow*) do not have additional disulfides. *Bottom set* represents typical spatial structures of three toxin groups as follows: long neurotoxin α-Ctx (PDB code 1CTX), short neurotoxin NT II (PDB code 1NOR), and nonconventional or weak toxin, here represented by the published structure of candoxin (PDB code 1JGK) that shares homology with WTX (*N. kaouthia* nonconventional toxin) and OWT (*N. oxiana* nonconventional toxin). Sequence alignments were produced via Clustal W algorithm; signal peptide sequences were removed manually, and *top line* shows numbering of α-Ctx residues. Backbones are shown in *gray*; β-strands are shown as *arrows*; cysteine residues, forming disulfide bonds are shown as *yellow sticks* on structures and highlighted *orange* in sequences, loop II arginine and valine residues in sequences are shown in *blue* and *green*, respectively.

and α9 (11) nAChR subunits were obtained in a complex with α-Bgt.

TFTs form an abundant group of proteins found in Colubridae, Elapidae, and Psammophiinae snake venoms. Members of this group possess no enzymatic activity and bind to receptors from different groups as follow: nAChRs (short and long chain α-neurotoxins), muscarinic acetylcholine receptors (African mamba-derived muscarinic toxins), L-type calcium channels (calciseptine from black mamba venom); and ASIC1, acid-sensitive ion channel (mambalgines). There are also three-finger cytotoxins (cardiotoxins) that interact with the cell plasma membrane (12).

Typical members of the long-chain group of TFTs, such as α-Bgt from *Bungarus multicinctus* as well as α-cobratoxin (α-Ctx) from *Naja kaouthia* cobra, neurotoxin NT I from *Naja oxiana,* and LsIII from marine krait *Laticauda semifasciata*, have an additional disulfide bond in loop II (Fig. 1, *bottom left*). This disulfide has been identified as a crucial feature for binding at the neuronal nAChR intersubunit sites (13, 14). Short neurotoxins, such as *Naja oxiana* neurotoxin II (NT II), acting exclusively on muscle nAChRs, do not have this additional disulfide (Fig. 1, *bottom center*). Another group, closely related to α-neurotoxins, is the group of so-called nonconventional or weak neurotoxins. In contrast to the previous two groups, weak toxins have an additional disulfide bond in the first loop (Fig. 1, *bottom right*), and show both weaker affinity toward nAChRs and some cross-reactions with other receptors (15). The toxins listed above block nAChRs with affinities that range from nanomoles to tens of micromoles/liter, and α-Bgt is the most active (Table 1). Interestingly, evidence for α-Ctx inhibition of T-type calcium channels through muscarinic receptors was recently provided (16), which may indicate that α-Ctx also has biological targets other than nAChRs.

TABLE 1

Affinities of different three-finger toxins toward nAChRs and acetylcholine-binding proteins

α7-nAChR is the human neuronal homopentameric nAChR, Tca-nAChR is the *Torpedo californica* muscle-type nAChR; Ac- and Ls-AChBP are *L. stagnalis* and *Aplysia californica* acetylcholine-binding proteins, respectively. ND means not determined.

Neurotoxin	IC_{50}			
	α7-nAChR	Tca-nAChR	Ac-AChBP	Ls-AChBP
		nM		
α-Ctx	105 (24)	4.5 (24)	356	250
α-Bgt	3	1	250 (46)	1.8
NTI	34 (14)	ND	1100	ND
WTX	3000 (15, 23)	14,800 (15, 23)	ND	ND
OWT	2000 (26)	30,000 (26)	ND	ND
NTII	≫10,000 (18, 25)	3 (18)	ND	ND

Fluorescent α-Bgt is widely used in applications concerning nAChR location and expression (17–19). Moreover, the "bungarotoxin-binding site" comprising a fragment of the α1 nAChR could be incorporated into the extracellular loops of different receptors allowing imaging of the receptors on the surface of living cells with the fluorescently labeled α-Bgt, which in particular also has been done for the GABA$_A$R (20, 21). Using fluorophore-conjugated α-Bgt, about a decade ago the first evidence of α-Bgt binding to GABA$_A$R was obtained (22). However, it was suggested to be limited to the peculiar β3/β3-binding sites, whose existence *in vivo* in the wild-type organisms has not been unambiguously demonstrated. This work aroused our interest in searching for novel GABA$_A$R ligands among snake venom components structurally similar to α-Bgt,

namely among various TFTs, as well as among α-conotoxins, another class of nAChR inhibitors.

Here, we report specific labeling of the α1β3γ2 subtype of $GABA_AR$ with a fluorescent derivative of α-Ctx, as well as inhibition of GABA-induced currents in a series of $GABA_ARs$ by well known TFTs belonging to different structural groups and exhibiting anticholinergic properties; interaction of α-conotoxin ImI with α1β3γ2 $GABA_AR$ was found as well.

Experimental Procedures

Three-finger Toxin Preparations—Ls III was from Latoxan (Valence, France). WTX, α-Ctx, and NT II were obtained as described previously (23–25) and OWT as described previously (26). NT I was obtained as described previously (27) with additional purification by reversed phase HPLC. α-Bgt was purified from *B. multicinctus* venom by combination of gel filtration, ion-exchange, and reverse-phase HPLC, and α-Bgt Val-31 analogue was used in this work. The structures of toxins obtained were confirmed by mass spectrometry. Chimeric NT II/I toxin with the tip of the second loop from NT I grafted to the NT II structure was obtained as described previously (14).

Peptide Chemical Synthesis—Peptide WCDAFCSIRGKR from the α-Ctx loop II and α-conotoxin ImI was synthesized as described previously (28).

Electrophysiology—Oocytes were obtained from healthy mature (>10 cm) *Xenopus* frogs. After manual separation, oocytes were injected with 2–3 ng of laboratory PCI vector containing DNA sequences encoding mouse $GABA_AR$ subunits. Oocytes were incubated at 18 °C in ND96 solution (5 mM HEPES/NaOH, pH 7.6, 96 mM NaCl, 2 mM KCl, 1.8 mM $CaCl_2$, 2 mM $MgCl_2$) supplemented with ampicillin and kanamycin. Recordings were performed 36–72 h after injections using turbo TEC-03X setup (npi electronic GmbH, Germany). During a typical experiment, agonist (γ-aminobutyric acid) was applied every 5 min. To evaluate the activity of the tested TFTs, they were pre-applied before the agonist and then co-applied with it. Incorporation of the γ2 subunit was confirmed by application of diazepam. Incorporation of δ subunit was confirmed using DS2 compound as described previously (29). Data are presented as mean ± S.E. and/or 95% confidence interval in parentheses.

Fluorescent α-Ctx—Coupling of Alexa Fluor 546 NHS reagent (Invitrogen) to α-Ctx was conducted according to the manufacturer's protocol. This fluorophore has been chosen due to similar spectral properties to commercially available Alexa Fluor 555 α-Bgt (Invitrogen) also used in this work.

Live Cell Imaging with Fluorescent Ligand—Mouse neuroblastoma Neuro2a cells grown in 96-well plates were transfected with laboratory PCI plasmids encoding $GABA_AR$ subunits and GFP-encoding plasmid (Evrogen, Russia) following the Lipofectamine transfection protocol (Invitrogen). Transfected cells were grown in DMEM (Paneco, Russia) supplemented with 10% fetal bovine serum (PAA Laboratories, Austria) at 37 °C in a CO_2 incubator for 48 h. The growth medium was removed; cells were rinsed with a buffer (20 mM HEPES, 140 mM NaCl, 2.8 mM KCl, 2 mM $CaCl_2$, 1 mM $MgCl_2$, 10 mM glucose, pH 7.4) and incubated with 50 nM Alexa Fluor 555-labeled α-Bgt (Invitrogen) or Alexa Fluor 546-labeled α-Ctx for 20 min at room temperature. In control experiments, 50-fold molar excess of nonlabeled α-Ctx was added to the incubation medium. The cells were then washed twice with the buffer and were visualized by an epifluorescent microscope (Olympus, Japan) using the appropriate filter combination. In competition experiments, 1–4000 μM muscimol or 400 μM diazepam were added to the incubation medium (140 mM NaCl, 2 mM $CaCl_2$, 2.8 mM KCl, 4 mM $MgCl_2$, 20 mM HEPES, 10 mM glucose, 1% BSA, pH 7.4) as described previously (19). Data were analyzed using the ImageJ program with the standard set of plugins (30). Fluorescence was quantified as follows: field of view was photographed in two channels as follows: one to detect fluorescent ligand and another to detect GFP. Background of images was subtracted, and maximum points were found on the GFP image and selected. Selection was enlarged to fit cells on the image and transferred to an image containing fluorescent ligand detection (same field of view); then the mean fluorescence was measured and normalized to the difference between total fluorescent binding and unstained cells fluorescence. In each well, 2–4 random fields of view were photographed, and each individual experiment included several wells; at least three independent experiments were performed.

Molecular Modeling—The extracellular domains of α and β subunits forming the β+α− interface of $GABA_AR$ were modeled using the atomic coordinates of the β3 extracellular domain taken from the recently published β3-homopentameric x-ray structure (2) and the extracellular domain of the α1 subunit, which was constructed via the Swiss model homology modeling service using the crystal structure of the β3 subunit from homo-oligomeric receptor as a template (31). $GABA_AR$ subunits share some homology with the *Lymnaea stagnalis* acetylcholine-binding protein (AChBP). Assuming that α-Ctx binds to $GABA_ARs$ in a way similar to the crystal structure of the α-Ctx-bound AChBP, we constructed models of α-Ctx complexes with $GABA_AR$ extracellular domains by aligning the β3 subunit extracellular domain with the principal AChBP subunit and α1 subunit extracellular domain with the complementary AChBP subunit from its x-ray structure with α-Ctx (PDB 1YI5) using UCSF Chimera (32). Resulting structures were energy-minimized with GROMACS 5.0 (33) and then treated with molecular dynamics procedure using OpenMM libraries (34) with the aid of AMBER force field parameters (35) and GBSA implicit solvent model to simulate 100 ns of complex behavior. Resulting coordinates were analyzed with VMD (36) and UCSF Chimera software.

Single-point Mutagenesis—The S67K and K67S mutations (in the α1 and α2 subunit, respectively) were obtained by PCR amplification of α1 and α2 subunits in the vector with the following primers: forward primer 5-gtgtttttccgccaaaagtggaaggatgaaagattaaaattc-3 and reverse primer 5-catccttccagctttggcggaaaaacacatctattg-3 (for S67K); forward primer 5-gctcgtctttccagctttgtcgaaagaaaacatctattg-3 and reverse primer 5-cttcgacaaagctggaaagacgagcggttaaaatttaaag-3 for (K67S) by using Phusion High-Fidelity DNA polymerase. Amplification product was analyzed after 25 cycles of the following thermal steps: 2 min of initial denaturation at 98 °C; 20 s of denaturation at 98 °C; 1 min of annealing at 65–70 °C; 3 min of extension at 72 °C, and 10 min of final extension at 72 °C. The product

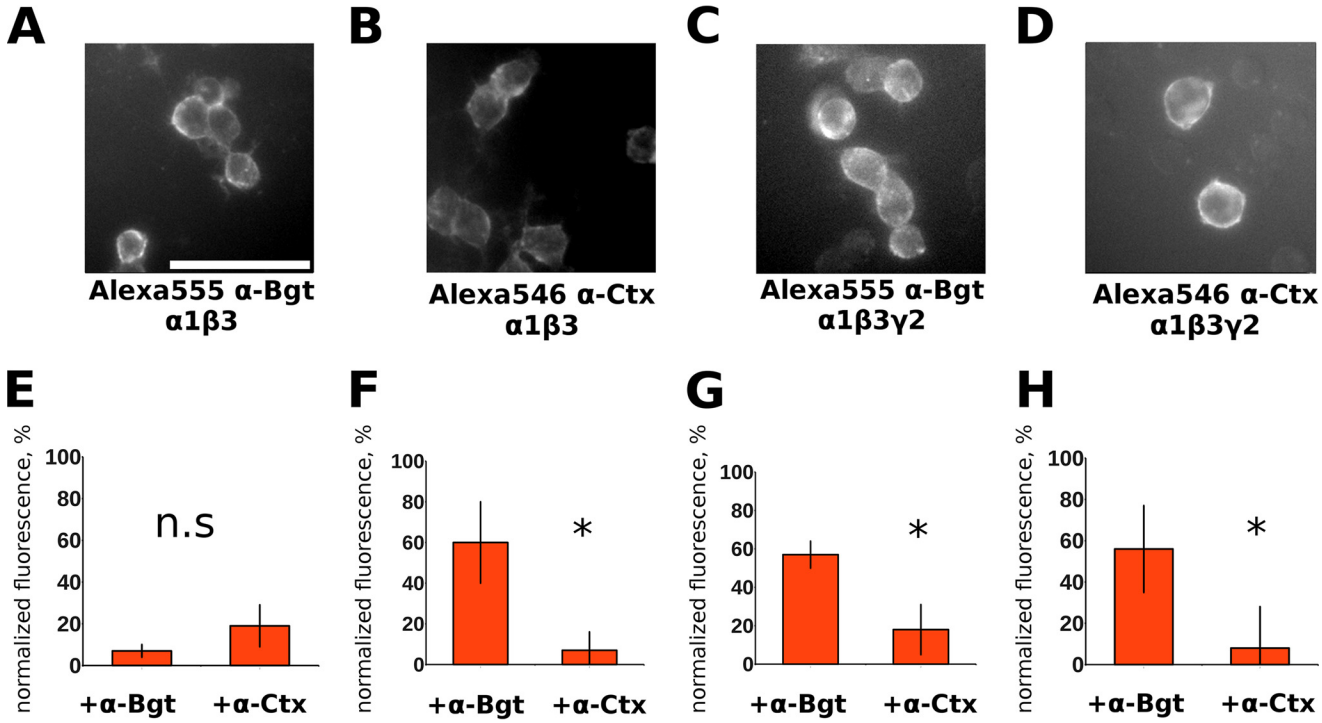

FIGURE 2. **Alexa Fluor 555 α-Bgt and Alexa Fluor 546 α-Ctx bind to the surface of cells expressing α1β3 or α1β3γ2 receptors and binding is differentially inhibited by α-Bgt and α-Ctx.** Alexa Fluor 555 α-Bgt (*A* and *C*) and Alexa Fluor 546 α-Ctx (*B* and *D*) binding to Neuro2a cells transfected with α1β3 (*A* and *B*) and α1β3γ2 (*C* and *D*) GABA$_A$R subunits (*scale bar*, 50 μm). *Bars* represent remaining fluorescence in the presence of α-Bgt or α-Ctx of α1β3 cells stained by Alexa Fluor 555 α-Bgt (*E*) or Alexa Fluor 546 α-Ctx (*F*). Note that Alexa Fluor 546 α-Ctx binding to α1β3-transfected cells was significantly ($p < 0.05$) better blocked by α-Ctx, whereas Alexa Fluor 555 α-Bgt binding was blocked with equal efficiency by both toxins. However, Alexa Fluor 555 α-Bgt (*G*) and Alexa Fluor 546 α-Ctx (*H*) binding to cells transfected with α1β3γ2 were blocked more effectively by α-Ctx ($p < 0.05$). Concentrations of fluorescent derivatives were 50 nM; the mixtures were incubated for 15 min, and then unbound ligand was washed out with buffer. Competition experiments using fluorescent derivatives and native α-Ctx and α-Bgt were performed by incubation of cells with unlabeled toxins at 5 μM along with addition of labeled analogues. The data were analyzed with ImageJ. Note that data are normalized to differences between mean stained and unstained cell fluorescence. Three independent experiments were performed for each data point. Data are presented as mean ± 95% confidence interval; differences were interpreted as significant ($p < 0.05$, *asterisk*) if intervals are not intersecting (if intervals intersect, difference was interpreted as nonsignificant, *n.s.*).

obtained was incubated with DpnI enzyme to restrict the methylated DNA and then transformed into XL1-Blue supercompetent cells. The mutations were confirmed by DNA sequencing.

Results

Long-chain α-Ctx and Naja oxiana α-Neurotoxin NT I Compete with Fluorescent α-Bgt for GABA$_A$R-binding Site—First of all, we decided to check whether α-Ctx could displace a fluorescent α-Bgt derivative from α1β3 GABA$_A$R. We reproduced (Fig. 2*A*) fluorescent Alexa Fluor 555 α-Bgt binding to (presumably) the β3/β3-interface of α1β3 receptors first reported by McCann *et al.* (22). α-Ctx at 5 μM concentration competed with fluorescent α-Bgt and displaced it almost completely from the receptor. Interestingly, *Naja oxiana* NT I (see Fig. 1 for sequence alignments) was also an effective competitor; it diminished Alexa Fluor 555 α-Bgt binding by 91 ± 2% (experiments not shown).

Fluorescently Labeled α-Ctx Can Be Used for Imaging of Live Cells Expressing GABA$_A$R—To study α-Ctx competition with α-Bgt in detail, we tested the applicability of a α-Ctx fluorescent derivative in cytochemical experiments for imaging of living cells heterologously expressing α1β3 and α1β3γ2 GABA$_A$R. α-Ctx bearing Alexa Fluor 546 fluorophore has been chosen due to similar spectral properties to commercially available Alexa Fluor 555 α-Bgt. It should be noted that we had no intention of registering simultaneously Alexa Fluor 555 α-Bgt and Alexa Fluor 546 α-Ctx binding. Both ligands (Alexa Fluor 555 α-Bgt and Alexa Fluor 546 α-Ctx) brightly stained cells expressing either α1β3 (Fig. 2, *A* and *B*) or α1β3γ2 subunit combinations (Fig. 2, *C* and *D*). The actual expression of the γ2-subunit in α1β3γ2 receptors was confirmed in patch clamp experiments with diazepam as discussed below (Fig. 4*A*). Binding of fluorescent toxins was then blocked by unlabeled toxins (α-Ctx or α-Bgt) to determine specificity of staining. Interestingly, only for α1β3-expressing cells stained by Alexa Fluor 555 α-Bgt (Fig. 2*E*), we detected no difference in efficiency of fluorescence block by 5 μM toxins (α-Bgt or α-Ctx). Fluorescence of α1β3-expressing cells stained by Alexa Fluor 546 α-Ctx, as well as α1β3γ2-expressing cells stained by either Alexa Fluor 555 α-Bgt or Alexa Fluor 546 α-Ctx, was more effectively blocked by 5 μM α-Ctx (Fig. 2, *F–H*).

Snake Venom Neurotoxins from Different Structural Groups Inhibit GABA$_A$R—To test whether α-Ctx and other toxins could inhibit α1β3γ2 GABA$_A$R, we performed two-electrode voltage clamp experiments. It was found that α-Ctx, as well as Ls III (long-chain α-neurotoxin from *Laticauda semifasciata*), and nonconventional toxin WTX from *Naja kaouthia* venom inhibit the GABA$_A$Rs in a dose-dependent manner (Fig. 3). Given at 10 μM Ls III and WTX blocked GABA-evoked response by 83 ± 12 and 31 ± 8%, respectively. Long-chain NT I and α-Bgt at 10 μM inhibited α1β3γ2 receptors only by 17 ± 5

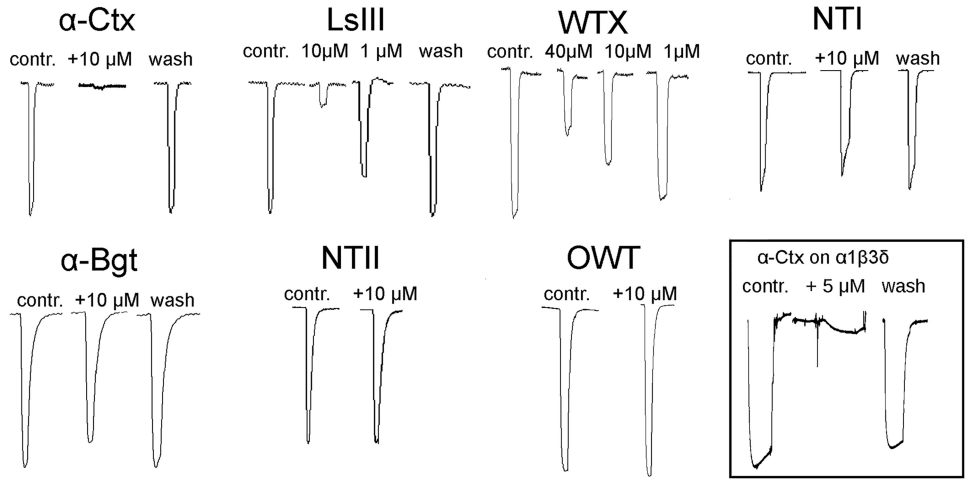

FIGURE 3. **Effects of different three-finger toxins on GABA-evoked currents.** Electrophysiological recordings demonstrate that three-finger toxins can inhibit GABA$_A$R. GABA was applied alone or co-applied with the indicated toxin to oocytes injected with cDNA encoding α1, β3, and γ2 subunits. First peak of each set represents control (*contr.*) with a 1-s application of 10 μM GABA alone, corresponding to EC$_{20-50}$; the concentration of co-applied toxin is indicated *above* the recording. The traces marked as *wash* represent the response to GABA after 5 min of oocyte washing with the buffer solution. The *lower right inset* shows inhibition of $\alpha1\beta3\delta$ receptor by α-Ctx at 5 μM.

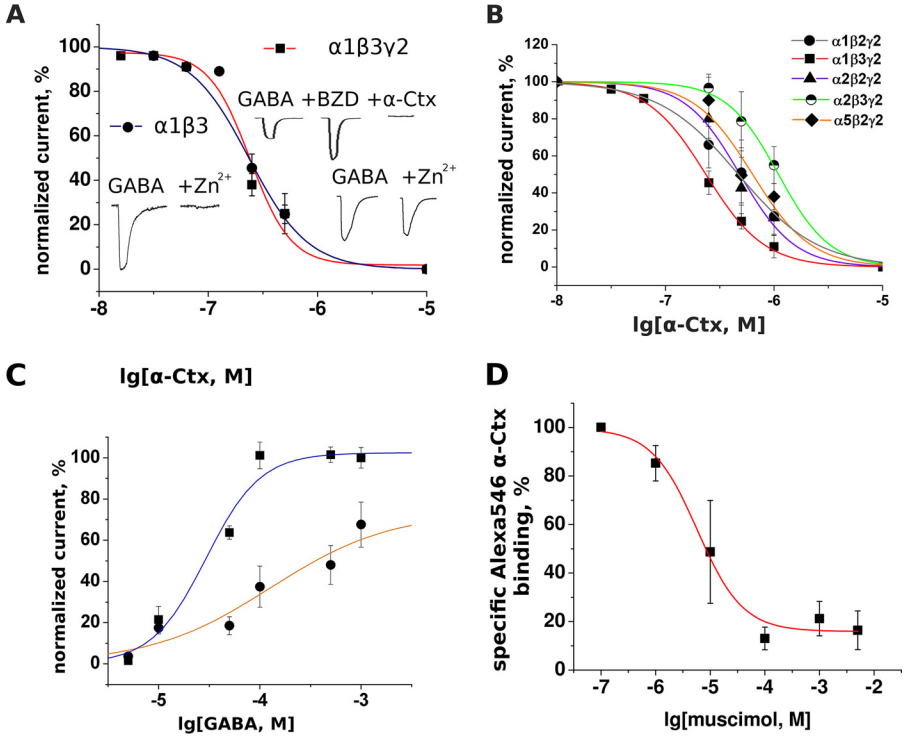

FIGURE 4. **Inhibition of different GABA$_A$R subtypes by α-Ctx and inhibition of Alexa Fluor 546 α-Ctx binding on $\alpha1\beta3\gamma2$ by muscimol.** *A,* inhibition of $\alpha1\beta3$ and $\alpha1\beta3\gamma2$ GABA$_A$Rs by α-Ctx. The presence of γ subunit is confirmed by the effect of the benzodiazepine 1 μM diazepam (*BZD*) and differential sensitivity to 50 μM Zn^{2+} (see *insets*). Absence of a γ subunit influence on α-Ctx inhibition is consistent with the assumption that the α-Ctx-binding site is located at an interface between α and β subunits. *B,* this toxin manifests modest subtype selectivity; it inhibits $\alpha1\beta3\gamma2$ receptor five times more potently than $\alpha2\beta3\gamma2$. The potency of α-Ctx against diverse sets of GABA$_A$R subunits was examined using the two-electrode voltage clamp method. To measure the effect of different α-Ctx concentration, α-Ctx was applied alone to the oocyte for 5 min before control GABA application and then was co-applied with GABA (10 μM, EC$_{20-50}$). Current amplitudes obtained in the presence of α-Ctx were expressed as percentage of control amplitudes and plotted against logarithm of toxin molar concentration. *C,* GABA dose-response curve at $\alpha1\beta3\gamma2$ receptors without α-Ctx (*upper curve*) and in the presence of 250 nM α-Ctx (*lower curve*). GABA EC$_{50}$ is shifted to the right and the Hill slope is reduced, suggesting noncompetitive or some mixed competitive/noncompetitive type of inhibition. *D,* muscimol competes with Alexa Fluor 546 α-Ctx on $\alpha1\beta3\gamma2$ GABA$_A$R suggesting α-Ctx-binding sites overlap with orthosteric sites located at the β/α interface. Fluorescence data were normalized to the difference between mean stained cell fluorescence and mean cell fluorescence blocked by 10 μM α-Ctx (*i.e.* data represent specific α-Ctx binding). Data were fitted to a dose-response equation using the Origin 7.5 software.

and 19 ± 3%, respectively. No inhibition was observed for short-chain neurotoxin NT II and nonconventional toxin OWT, both from *N. oxiana* venom, at concentrations of 10 μM. Interesting, α-Ctx (5 μM) also inhibited $\alpha1\beta3\delta$ receptor (Fig. 3).

To characterize more broadly the α-Ctx potency and selectivity, we tested it on GABA$_A$R with different subunit combinations. First of all, we investigated the potency of α-Ctx for inhibition of GABA-induced currents at $\alpha1\beta3$ and $\alpha1\beta3\gamma2$

receptors. As expected, GABA-induced currents at $\alpha1\beta3$ receptors were completely inhibited by 50 μM Zn^{2+} in contrast to those at $\alpha1\beta3\gamma2$ receptors (Fig. 4*A*, *insets*). The incorporation of a $\gamma2$ subunit in $\alpha1\beta3\gamma2$ receptors was further demonstrated by their sensitivity to 1 μM diazepam. Interestingly, α-Ctx was able to completely inhibit diazepam-stimulated GABA currents, again demonstrating that α-Ctx is able to also block the actions of $\alpha1\beta3\gamma2$ receptors (Fig. 4*A*, *insets*). As shown in Fig. 4*A*, α-Ctx exhibited a comparable potency for inhibition of these two receptor subtypes, indicating that the $\gamma2$ subunit does not influence the potency of α-Ctx.

Then we investigated the effects of α-Ctx at $\alpha1\beta2\gamma2$, $\alpha1\beta3\gamma2$, $\alpha2\beta2\gamma2$, $\alpha2\beta3\gamma2$, and $\alpha5\beta2\gamma2$ receptors (Fig. 4*B*). α-Ctx exhibited a differential potency for inhibition of GABA-induced currents at the individual $GABA_A$ receptor subtypes. IC_{50} values for each of them are shown in Table 2. The potency of α-Ctx depended on the types of α and β subunits present in the receptor, supporting the conclusion that the α-Ctx-binding site is located at an interface between α and β subunits. In contrast to the strong inhibition of $\alpha1\beta3\gamma2$, long-chain Ls III (10 μM) inhibited $\alpha5\beta2\gamma2$ and $\alpha2\beta2\gamma2$ only by 13 ± 5 and 39 ± 9%, respectively (experiments not shown).

Electrophysiology Measurements Indicate That α-Ctx Inhibits GABA$_A$R in a Mixed Competitive/Noncompetitive Manner—To shed light on the α-Ctx mode of inhibition, we compared the GABA dose-response dependence (for $\alpha1\beta3\gamma2$ subtype) in the presence of 250 nM α-Ctx, a concentration that is sufficient to inhibit receptor response to 10 μM GABA by about 50% as compared with control (Fig. 4*C*). GABA EC_{50} value was shifted from 29 ± 7 to 128 ± 25 μM in the presence of α-Ctx. After looking at the individual data points, however, it seems that α-Ctx caused a parallel shift of the GABA dose-response curve in at least two steps. Such behavior would be consistent with a competitive inhibition of GABA binding by α-Ctx, when binding of α-Ctx to one of the two orthosteric sites caused an allosteric reduction of the GABA affinity for the second orthosteric site.

At 1 mM GABA, however, the current induced in the presence of toxin is 40% smaller than in its absence (Fig. 4*C*). Although the data do not allow a firm conclusion because the GABA concentration-response curve in the presence of toxin is not yet saturated at this concentration, they are consistent with an additional noncompetitive inhibition of GABA currents by α-Ctx (see below).

Muscimol but Not Diazepam Competes with Alexa Fluor 546 α-Ctx—We investigated whether diazepam, a classical benzodiazepine that binds at the α/γ interface (37), or the agonist muscimol that binds at the β/α interface can compete with Alexa Fluor 546 α-Ctx for binding to Neuro2a cells expressing $\alpha1\beta3\gamma2$ $GABA_AR$. Indeed, 200 μM muscimol reduced fluorescence by about 80% (Fig. 4*D*), whereas diazepam had no effect at concentrations up to 400 μM (experiments not shown). These data support the conclusion that Alexa Fluor 546 α-Ctx to a large extent binds to the GABA-binding site of $GABA_A$ receptors. The remaining 20% of bound Alexa Fluor 546 α-Ctx cannot be displaced by muscimol, suggesting that this binding of α-Ctx occurs via a site different from the orthosteric binding site.

α-Cobratoxin Loop II Peptide (WCDAFCSIRGKR) and α-Conotoxin ImI Selective for α7 nAChR but Not the α-Conotoxins SIA and MII Selective for Muscle Type nAChR and Heteromeric Neuronal nAChRs, Respectively, Inhibit α1β3γ2 GABA$_A$R—We hypothesized that other polypeptide nAChR ligands could also inhibit $GABA_AR$ and chose α-conotoxin ImI because it was reported previously that ImI shares some structural features of the α-Ctx loop II (28). ImI binds efficiently to $\alpha7$ nAChR, *i.e.* to neuronal homopentameric nAChR, whereas α-Ctx in addition to $\alpha7$ nAChR also binds to muscle type

TABLE 2

EC_{50} values for GABA and IC_{50} values for α-Ctx at different combinations of $GABA_AR$ subunits

Subunit combination	EC_{50} ± S.E. (95% confidence interval)	IC_{50} ± S.E. (95% confidence interval)
	μM	nM
$\alpha1\beta2\gamma2$	35 ± 1 (33, 36)	469 ± 23 (427, 515)
$\alpha1\beta3\gamma2$	29 ± 7 (19, 44)	236 ± 7 (223, 250)
$\alpha2\beta2\gamma2$	45 ± 1 (43, 47)	485 ± 39 (417, 564)
$\alpha2\beta3\gamma2$	12 ± 1 (11, 13)	1099 ± 57 (1016, 1088)
$\alpha5\beta3\gamma2$	20 ± 2 (17, 24)	635 ± 91 (489, 825)

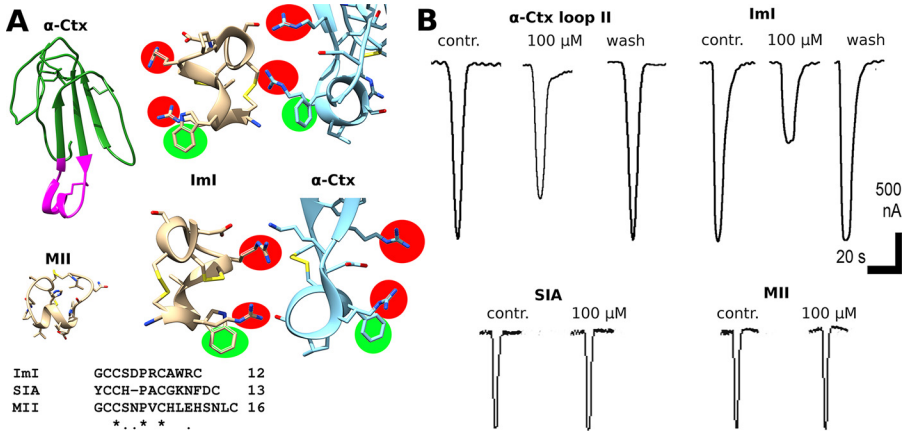

FIGURE 5. *A*, structural similarity of α-conotoxin ImI, selective for $\alpha7$ nAChR, to the tip of the α-Ctx loop II (*magenta*). Note that two positively charged arginines (highlighted *red*) are exposed in a very similar manner with respect to aromatic residues (tryptophan or phenylalanine, highlighted *green*) in both ImI (shown *wheat*) and loop II of α-Ctx (shown *blue*). Two different views (*1st* and *2nd rows*) are provided for convenience. Amino acid sequences of α-conotoxins SIA and MII differ greatly from that of ImI (*bottom*). *B*, chemically synthesized WCDAFCSIRGKR peptide that mimics tip of α-Ctx loop II and α-conotoxin ImI at 100 μM inhibits 10 μM GABA-evoked current (*upper left* and *right traces*, respectively). SIA specific for muscle type nAChR and MII specific for heteromeric neuronal nAChR have no effect on the currents at 100 μM.

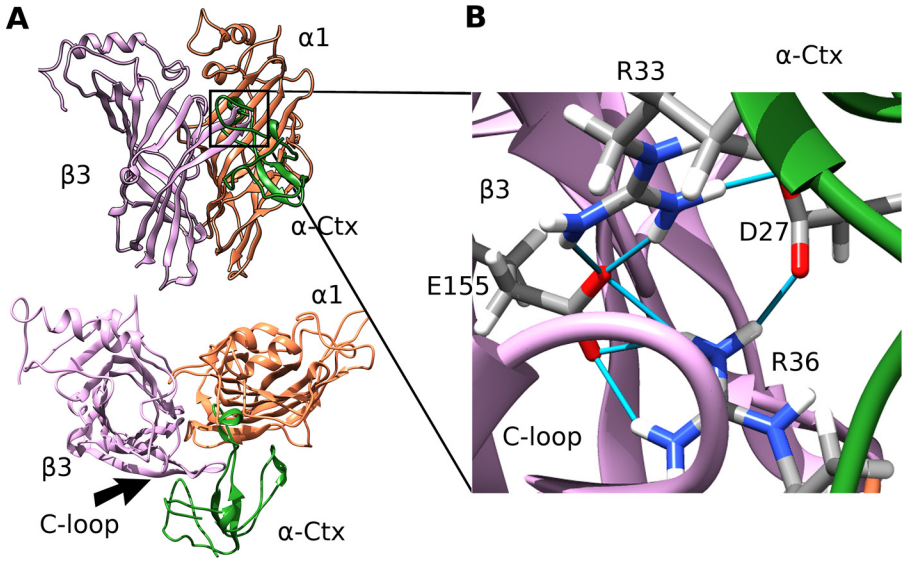

FIGURE 6. **Molecular modeling of α-Ctx binding to the GABA$_A$R.** *A,* side and top view of the molecular model of complex formed by α-Ctx with the orthosteric site of the GABA$_A$R. Toxin (*green*) rests under loop C of the β3 (*plum*) subunit. GABA$_A$R α1 subunit is colored *coral*. *B,* Arg-33 and Arg-36 from the α-Ctx loop II form a network of hydrogen bonds (shown as *light blue sticks*) with both α-Ctx Asp-27 and Glu-155 of the β3 subunit.

nAChR. We decided to test two other conotoxins: SIA that binds to muscle nAChR and MII that binds to neuronal non α7 nAChRs. α-Conotoxin ImI (see Fig. 5*A* for structure) inhibited the α1β3γ2 GABA$_A$R at 100 μM by 45 ± 5% in terms of GABA-evoked peak current (Fig. 5*B*). α-Conotoxins SIA and MII failed to show inhibition of GABA$_A$R at 100 μM (Fig. 5*B, bottom*). This experiment also proves specificity of inhibition, and because 100 μM is a rather high concentration, we had to make some control experiments with peptides chemically similar to ImI at such a high concentration.

We also performed experiments with the synthetic peptide WCDAFCSIRGKR comprising the tip of α-Ctx loop II. Synthetic fragment (see Fig. 5*A* for structure) inhibited the α1β3γ2 GABA$_A$R at 100 μM by 28 ± 10% in terms of GABA-evoked peak current, respectively (Fig. 5*B*). The above results suggest that new peptide ligands of GABA$_A$Rs could be found among toxins sharing common structural features with α-Ctx loop II.

α-Cobratoxin at Concentrations of Up to 40 μM Does Not Inhibit Homopentameric Glycine Receptor—Glycine receptor is another example of abundantly expressed Cl^--permeable Cys-loop receptors. It also shares very high sequence homology with GABA$_A$R subunits. To check whether α-Ctx possesses some activity against this receptor, we tested its activity against the human homopentameric α1 glycine receptor. At concentrations up to 40 μM, α-Ctx failed to inhibit glycine-evoked currents (data not shown). Thus, α-Ctx blocks GABA$_A$Rs but not the glycine receptor. However, it should be noticed that there are other subsets of glycine receptor (α2–3 and β) that were not tested.

Model for GABA$_A$R·α-Ctx Complex—GABA$_A$R spatial structure (2) has a very high degree of similarity to structures of AChBPs and extracellular nAChR domains for which the α-neurotoxin-binding sites were defined. Based on these data, we assumed that a complex of α-Ctx with the GABA$_A$R might resemble published structures of α-neurotoxins bound to AChBP or to the extracellular nAChR domain. Under this assumption, we suggested that loop II of α-Ctx might find its place under the loop C of the GABA$_A$R receptor subunit. To get a picture of such a hypothetical intersubunit binding site, we constructed homology models of extracellular domains of α1 GABA$_A$R subunits using the recently published structure of GABA$_A$R β3-homopentamer (2) as a template. Then a molecular model of the β3/α1 dimer with α-Ctx introduced under loop C of the β3 subunit was constructed by superimposition and alignment of the β3 extracellular domain structure with that of the AChBP protomer (PDB code 1YI5). The structure obtained was subjected to 100 ns of molecular dynamics. The last 40-ns complex was stable, and its backbone root mean square deviation did not exceed 0.1 nm. By the end of simulation, the complex retained the overall "TFT to Cys-loop" binding mode known from the x-ray structures (Fig. 6*A*) with the toxin loop II buried under loop C of the receptor. Interestingly, α-Ctx residues Arg-33 and Arg-36 form a stable network of salt bridges with both Asp-27 and β3 Glu-155 (Fig. 6*B*), which was present during all simulation times. The toxin C-terminal region and tips of loop I and loop II also formed contacts with both dimer subunits.

Electrophysiological Analysis of Chimeric NT II/I—To verify the model, we decided to test whether the loop II of the toxins plays a crucial role in functional inhibition of GABA$_A$R. In previous studies, short-chain toxin NT II with grafted loop II from long neurotoxin I was used to study the role of loop II in α-neurotoxin interaction with neuronal nAChRs (14). We used the same chimera in electrophysiological experiments on GABA$_A$R. Short-chain toxin NT II at 10 μM did not show any inhibition of the receptor but gained the inhibitory activity upon the grafting of loop II from long neurotoxin NT I (Fig. 7*A*). Chimeric NT II/I toxin and NT I generated a comparable inhibition of α1β3γ2 receptors (16 ± 3 and 19 ± 3%, respectively, Fig. 7*B*). Molecular dynamics simulations indicated that the model of NT II was unable to form a complex with the GABA$_A$R orthosteric intersubunit site in the manner similar to α-Ctx

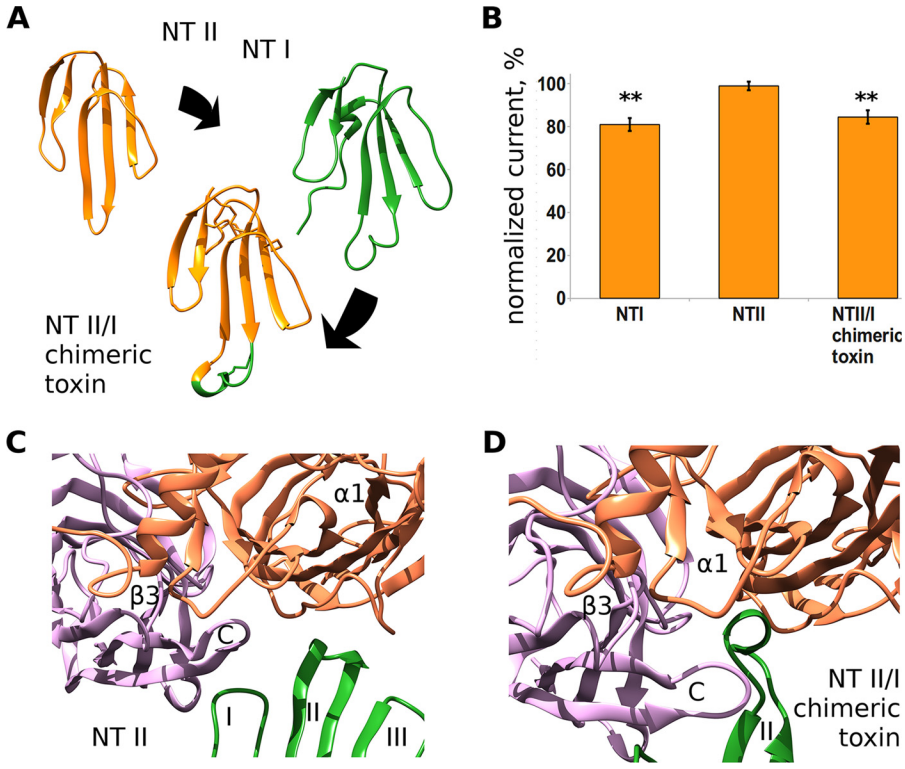

FIGURE 7. **Delineation of the active site in TFTs interacting with GABA$_A$Rs.** *A,* loop II peptide fragment CDAWCGS of NT I was grafted to NT II structure, replacing the corresponding SDH sequence (see Fig. 1 for sequence alignment). *B,* normalized GABA-evoked currents (10 μM of GABA, $\alpha1\beta3\gamma2$ GABA$_A$R) in the presence of wild-type NT I, NT II, and chimeric NT II/I at 10 μM. Wild-type NT II does not inhibit the receptor, whereas both wild-type NT I and NT II/I chimeric toxin show current inhibition by 19 ± 3 and 16 ± 3%, respectively. *Asterisks* indicate significant inhibition ($p < 0.01$, $n = 6$, paired *t* test). *C,* last frame of a 100-ns run of molecular dynamics simulation of NT II complex with $\beta3/\alpha1$ extracellular domains. NT II failed to reproduce mode of binding shown by α-Ctx model. *D,* molecular model of chimeric NT II/I toxin complex with $\beta3/\alpha1$ extracellular domains. Note that the tip of the loop II (which was grafted to the short toxin NT II molecule from long NT I toxin) rests under the C loop of $\beta3$ subunit.

(Fig. 7*C*). In contrast, the model of NT II/I formed a stable complex with loop II resting under the C-loop of $\beta3$ extracellular domain model (Fig. 7*D*).

Single Point Mutations α1(S67K) and α2(K67S) Located at the Complementary Surface of the Respective α-Subunit Change Inhibition by α-Ctx—Because we observed modest α-Ctx selectivity toward $\alpha1\beta3\gamma2$ (Table 2), we decided to test our model by introduction of $\alpha1\rightarrow\alpha2$ and $\alpha2\rightarrow\alpha1$ point mutations. Loop II of the toxin carries a significant positive charge, and we hypothesized that addition or deletion of a positive charge at position 67 of $\alpha1$ and $\alpha2$ subunits, located in close vicinity to the hypothetical toxin-binding site and occupied by a serine residue (Fig. 8*A*), might diminish affinity to α-Ctx in the $\alpha1$(S67K) mutant and increase affinity toward $\alpha2$(K67S) mutant. Indeed, we found that the α-Ctx IC_{50} value for $\alpha1$(S67K)$\beta3\gamma2$ GABA$_A$R (703 ± 39 nM) is closer to the $\alpha2$-containing receptor (1099 ± 57 nM, Table 2) than the $\alpha1$-containing receptor (236 ± 7 nM, Table 2), and vice versa the α-Ctx IC_{50} value for $\alpha2$(K67S)$\beta3\gamma2$ GABA$_A$R (442 ± 54 nM) is closer to the $\alpha1$-containing receptor than the $\alpha2$-containing receptor (Fig. 8*B*). At the same time GABA EC_{50} values were not affected by these mutations.

Discussion

There has been considerable progress in understanding the structure and function of GABA$_A$Rs (38). Notwithstanding, there are still significant gaps in our knowledge on peptide and proteins interacting with GABA$_A$Rs. In general, polypeptide ligands manifest higher selectivity to particular receptor subtypes as compared with low molecular weight organics. Several polypeptides interacting with GABA$_A$R have been reported earlier that include α-Bgt (22), diazepam-binding inhibitor protein, and its processing fragments such as the octadecaneuropeptide (39, 40). Given a plethora of different GABA$_A$R subunits, it seems surprising that there is such a paucity of known proteins interacting with the receptor. For example, a great deal of polypeptide toxins is known for nAChR, closely related to GABA$_A$R. Here, for a series of GABA$_A$R subtypes, we report specific fluorescent labeling and inhibition of GABA-induced ion currents by several protein toxins from snake venoms.

As a starting point, we reproduced α-Bgt binding to the $\alpha1\beta3$ GABA$_A$R reported in Ref. 22 to obtain a verified test system of binding. As expected, long-chain α-neurotoxin α-Ctx, closely related to α-Bgt, showed competition with α-Bgt binding. We then investigated whether a fluorescently labeled α-Ctx, could stain cells expressing $\alpha1\beta3\gamma2$ or $\alpha1\beta3$ GABA$_A$R. We found that Alexa Fluor 546 α-Ctx, as well as Alexa Fluor 555 α-Bgt, were able to stain both types of cells (Fig. 2, *A–D*). Whereas α-Ctx blocks Alexa Fluor 555 α-Bgt binding at $\alpha1\beta3$-transfected cells (Fig. 2*E*) as effectively as α-Bgt, Alexa Fluor 555 α-Bgt or Alexa Fluor 546 α-Ctx staining of $\alpha1\beta3$- or $\alpha1\beta3\gamma2$-transfected cells was blocked more effectively by α-Ctx (Fig. 2, *F–H*). This observation suggests that GABA$_A$Rs with different subunit combinations bear binding sites with slightly different properties.

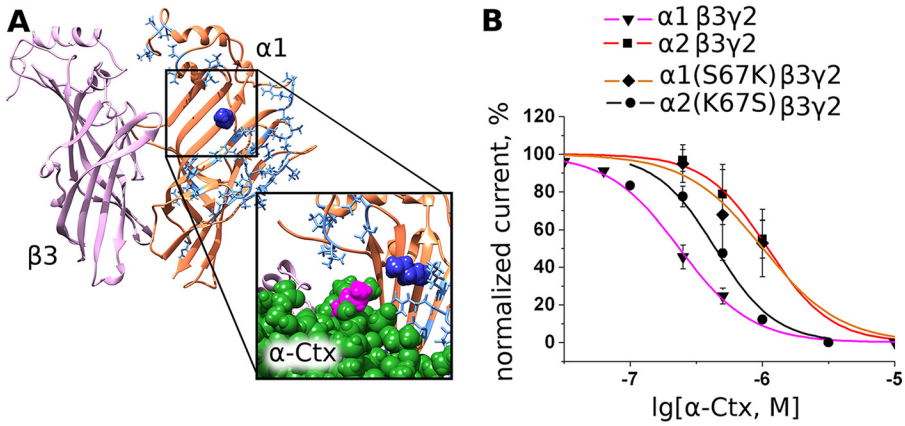

FIGURE 8. **Influence of GABA$_A$R single point mutation on α-Ctx binding.** *A,* extracellular domains of subunits forming β3/α1 interface. Residues that are different in α1 and α2 subunits are shown *blue* (*stick* representation), whereas α1 structure conserved between these two subunits is colored *orange*. Note that one of the closest to agonist-binding site residues is Ser-67 (*dark blue*). *Inset* shows that, according to our molecular modeling, by being mutated to lysine (as in α2 subunit) this residue comes close to the lysine of the α-Ctx loop II (*magenta*, space-filling model). *B,* inhibition of mutant receptor α1(S67K)β3γ2 by α-Ctx is characterized by a higher IC_{50} = 703 nM (632, 781 nM) value than wild-type α1β3γ2. However, inhibition of mutant receptor α2(K67S)β3γ2 by α-Ctx is characterized by a lower IC_{50} = 442 nM (352, 554 nM) value than wild-type α2β3γ2 suggesting the importance of β/α interface. GABA was given at 10 μM, which is slightly less than EC_{50}. Data points are expressed as percentage of control amplitudes (mean peak current ± S.E.).

To investigate how α-Ctx and other anticholinergic TFTs might influence GABA$_A$R function, we performed electrophysiology studies of α1β2γ2, α1β3γ2, α2β2γ2, α2β3γ2, α5β2γ2, and α1β3δ GABA$_A$R subunit sets expressed in *Xenopus* oocytes. It was found that α-Ctx blocks α1β3γ2 with a relatively high potency (IC_{50} = 236 nM, Fig. 4, *A* and *B*) and other receptor subtypes with lower potencies, namely in submicromolar to low micromolar range (Fig. 4*B*). It is worth noting that α-Ctx manifests some selectivity toward α1 as compared with the α2 subunit only in the presence of the β3 subunit, whereas in the presence of the β2 subunit it does not show noticeable selectivity to any α subunit investigated. This suggests that the α-Ctx-binding site might be located at the interface between the β and α subunit. Other tested TFTs were less active, and their potencies were not measured. However, it is clear that Ls III and WTX are active in the micromolar range, whereas NT II and OWT do not show any inhibition of α1β3γ2 receptor at 10 μM.

Electrophysiology measurements indicated that α-Ctx (for the α1β3γ2 subtype) shifted GABA dose-response curve to the right, at the same time changes in the slope and maximally achieved current were observed (Fig. 4*C*). Such a picture is typical of noncompetitive antagonists. However, we found that muscimol, acting as agonist of GABA$_A$R, but not the allosteric modulator diazepam, displaced Alexa Fluor 546 α-Ctx from α1β3γ2-transfected cells (Fig. 4*D*) to the level of ~20%. So a large part of α-Ctx action seems to be competitive and to be mediated via binding to the GABA-binding sites of GABA$_A$ receptors. Because occupation of only one orthosteric site is sufficient for receptor activation, the α-Ctx could bind either to one orthosteric site (as a competitive inhibitor) and allosterically inhibit receptor activation through the second site or α-Ctx could bind to both orthosteric and allosteric types of sites, shifting GABA dose-response curve and diminishing maximal current amplitude. The second possibility is supported by the finding that about 20% of bound Alexa Fluor 546 α-Ctx could not be displaced by muscimol, supporting an additional interaction of Alexa Fluor 546 α-Ctx with a nonorthosteric binding site.

The tip of loop II is the most important part of α-Ctx and other TFTs for binding to AChBP and nAChRs (41). To test whether this region is also involved in the interaction with GABA$_A$R, we applied mutant NT II with loop II grafted from NT I. This chimeric toxin (14) seems to be a suitable candidate because we have not detected any inhibition of GABA$_A$R by NT II at 10 μM, but we observed some inhibition by NT I at the same concentration. Upon grafting of the NT I loop II fragment bearing a disulfide loop to the short neurotoxin NT II, the latter became functionally active against the receptor, strongly supporting the key role of loop II in TFTs in the interaction with GABA$_A$R. Thus, we conclude that the tip of the loop II of TFTs plays a crucial role in GABA$_A$R binding and inhibition.

Previously, it was suggested that some structural similarity (see Fig. 5*A*) of α-conotoxin ImI to the α-Ctx loop II may contribute to its binding to the neuronal nAChRs (28). Electrophysiology revealed that ImI inhibited GABA$_A$R at 100 μM (Fig. 5*B*), whereas muscle nAChR-specific SIA and heteromeric nAChR-specific MII, lacking α-Ctx-similar features, were ineffective (Fig. 5*B, bottom*). Therefore, even molecules with structural similarity to the α-Ctx loop II could inhibit GABA$_A$R. These data indicated that α-conotoxin ImI represents another type of polypeptide compounds able to interact with GABA$_A$R. Moreover, synthetic peptide representing the sequence WCDAFCSIRGKR of the α-Ctx loop II tip also inhibited GABA$_A$R (Fig. 5*B*). Despite the fact that we observe only weak inhibition at a relatively high concentration, short peptide GABA$_A$R ligands on the base of loop II peptide or ImI could represent a good starting point for rational design of more specific ligands.

Our findings suggest that α-Ctx binds at the β/α interface and the loop II tip plays a crucial role in its binding. Given that, we constructed a molecular model of α-Ctx bound to the β3/α1 dimer of extracellular domains and performed 100-ns molecular dynamics studies in implicit solvent. Loop II residues 25–36 rested stably at the site under the loop C of the β3 subunit (Fig. 6*A*). With respect to β3 subunit backbone, root mean square deviation of these residues have not exceeded 0.15 nm, suggest-

ing that such a complex might exist in principle. Interestingly, we found that both Arg-33 and Arg-36 residues in α-Ctx form salt bridges with α-Ctx Asp-27 and β3 Glu-155 (Fig. 6*B*). Arg-36 residue is unique to α-Ctx among all tested toxins, and its substitution by hydrophobic residues in other toxins (Fig. 1) could explain their weaker GABA$_A$R inhibiting activity. Molecular modeling of NT II interaction with the β3/α1 dimer revealed inability of this short toxin to form a complex with the orthosteric site of GABA$_A$R (Fig. 7*C*). In contrast, a molecular model of the NT II/I chimeric toxin showed properties very close to that of α-Ctx complex model with the β3/α1 dimer. In particular, loop II, grafted to the NT II scaffold from NT I, formed stable contacts with the C-loop of the β3 subunit extracellular domain (Fig. 7*D*).

It should be noted that previously we demonstrated that upon modification of α-Ctx with NHS ethers, the major product is the one with the label attached at Lys-23 (42). This lysine residue is in loop II, which according to our model takes part in receptor binding. However, it is not one of the deeply buried residues, and its modification does not necessarily disrupt α-Ctx binding, as indicated by the interaction of modified α-Ctx with the nAChRs (42).

In electrophysiological studies, we observed a somewhat more potent inhibition of α1β3γ2 over α2β3γ2 GABA$_A$R. Because both α1 and α2 subunits share extremely high sequence homology, the respective receptors should differ only slightly in their extracellular parts. To test the above-described model, as a candidate for single-point mutagenesis we chose the Ser-67 residue (numbering of residues is given according to the homology model of extracellular domain) situated at the β/α1 interface. It is substituted by a lysine residue in the α2 subunit, and this positively charged residue could confer the difference in the α-Ctx affinity toward these two receptors, because α-Ctx loop II bears significant positive charge itself. This mutation was done, and the α-Ctx potency at α1(S67K)β3γ2 GABA$_A$R was diminished, approaching that at α2β3γ2 (Fig. 8).

When our manuscript was ready for submission, two papers (43, 44) appeared, clearly demonstrating the perspective of TFTs for research on GABA$_A$Rs. In Ref. 43, the authors analyzed in detail the interactions of α-Bgt and its fluorescent derivative with GABA$_A$R in hippocampal neurons and with recombinant GABA$_A$R subtypes, comparing their effects on ion currents and staining patterns in the presence of diverse ligands (agonists and antagonists) both with GABA$_A$Rs and nAChRs. Their conclusion was that α-Bgt inhibits various functional GABA$_A$R subtypes with different efficiency, with the α2β2γ2 receptor being inhibited most potently. Here, we show that the preferred target of α-Ctx is the α1β3γ2 receptor, indicating that diverse α-neurotoxins may have different affinity for distinct GABA$_A$R subtypes and might be able to distinguish between various GABA$_A$R subtypes. Concerning the mode of α-Bgt binding, Hannan *et al.* (43) described it as "a mixed inhibitory manner." It is quite clear that further work is necessary to obtain a high resolution picture for recognition of GABA$_A$R by both α-Bgt and α-Ctx.

Interestingly, in Ref. 43 it was also found that α-Bgt inhibited spontaneous channel openings in GABA$_A$R composed of α4 and δ subunits, but in the presence of GABA the toxin behaved as a positive allosteric modulator. Such effects were not observed in this study, supporting our observation (Fig. 2) that different toxins, dependent on the receptor composition, might exhibit different effects. However, α-Bgt was found to bind at the orthosteric site (43). It is thus possible that binding of toxins to one of two orthosteric sites could lead to an allosteric change in the conformation of the second site and that the functional consequences of these allosteric interactions might be influenced by the type of additional (in this case δ and γ) subunits in the receptor (45).

The second above-mentioned paper (44) also deals with GABA$_A$R potentiators by describing two TFTs from the coral snake venom that potentiate the GABA$_A$R activity at low nanomolar concentrations. An undisputable advantage of these toxins is that they do not act on nAChRs and are the first, strictly speaking, GABA$_A$R-specific TFTs. These toxins (MmTX1 and MmTX2) are not α-neurotoxins (like α-Ctx or α-Bgt) but belong to the nonconventional neurotoxins (additional 5th disulfide in loop I) like the GABA$_A$ receptor inhibiting toxin WTX identified in our study (Fig. 3). We and the authors of Ref. 44 hypothesized that TFTs should bind to GABA$_A$R in a similar manner as α-neurotoxins bind to nAChRs. This is supported by their finding that the toxin interaction is decreased upon the H33S mutation in the central loop II of MmTX2 or upon double mutation G228E/Q231K in the receptor loop C. Concerning the binding interface of the toxin, this single mutation agrees with the conclusions we made based on the activity of the chimeric TFT. Our S67K and K67S mutations in the α1 and α2 subunits of GABA$_A$R, respectively, although not being in the loop C, also affect binding, and it is clear that mapping of the toxin-binding interfaces in the GABA$_A$R is a challenging task.

In conclusion, even such extensively studied objects as α-Ctx, which has been investigated since the 1970s, could hide some secrets, as demonstrated by its earlier overlooked inhibition of GABA$_A$Rs. We showed that α-Ctx and NT I compete with α-Bgt for binding site(s) at the α1β3 receptor, and we found that α-Ctx, LsIII, and WTX inhibit the functional activity of α1β3γ2 GABA$_A$R in the submicromolar to micromolar concentration ranges. In addition, the first peptide toxin α-conotoxin ImI inhibiting GABA$_A$R was identified. These facts together with previously published observations demonstrate that GABA$_A$Rs are the target for α-conotoxin and diverse three-finger toxins.

Author Contributions—V. I. T., W. S., and Y. N. U. made study concepts and design. D. S. K., I. V. S., L. V. S., L. O. O., E. V. K., E. N. L., D. A. D., M. N. Z., I. A. I., I. E. K., V. G. S. and J. R. designed, performed, and analyzed the experiments and interpreted the data. D. S. K., I. V. S., E. N. L., L. O. O., and E. V. K. wrote the manuscript. M. N. Z., I. A. I., and V. G. S. provided technical assistance. W. S., V. I. T,. and Y. N. U. revised the manuscript critically for important intellectual content and made a final approval of the version to be published. All authors reviewed the results and approved the final version of the manuscript.

Acknowledgment—We thank Dr. Christoph Methfessel for help with electrophysiology measurements.

References

1. Krishek, B. J., Moss, S. J., and Smart, T. G. (1996) Homomeric β1 γ-aminobutyric acid A receptor-ion channels: evaluation of pharmacological and physiological properties. *Mol. Pharmacol.* **49,** 494–504
2. Miller, P. S., and Aricescu, A. R. (2014) Crystal structure of a human $GABA_A$ receptor. *Nature* **512,** 270–275
3. Olsen, R. W. (2006) Picrotoxin-like channel blockers of $GABA_A$ receptors. *Proc. Natl. Acad. Sci. U.S.A.* **103,** 6081–6082
4. Wyrembek, P., Negri, R., Appendino, G., and Mozrzymas, J. W. (2012) Inhibitory effects of oenanthotoxin analogues on GABAergic currents in cultured rat hippocampal neurons depend on the polyacetylenes' polarity. *Eur. J. Pharmacol.* **683,** 35–42
5. Razet, R., Thomet, U., Furtmüller, R., Jursky, F., Sigel, E., Sieghart, W., and Dodd, R. H. (2000) Use of bicuculline, a GABA antagonist, as a template for the development of a new class of ligands showing positive allosteric modulation of the $GABA_A$ receptor. *Bioorg. Med. Chem. Lett.* **10,** 2579–2583
6. Ashton, H. (2005) The diagnosis and management of benzodiazepine dependence. *Curr. Opin. Psychiatry* **18,** 249–255
7. Kasheverov, I. E., Utkin, Y. N., and Tsetlin, V. I. (2009) Naturally occurring and synthetic peptides acting on nicotinic acetylcholine receptors. *Curr. Pharm. Des.* **15,** 2430–2452
8. Berg, D. K., Kelly, R. B., Sargent, P. B., Williamson, P., and Hall, Z. W. (1972) Binding of α-bungarotoxin to acetylcholine receptors in mammalian muscle. *Proc. Natl. Acad. Sci. U.S.A.* **69,** 147–151
9. Clarke, P. B., Schwartz, R. D., Paul, S. M., Pert, C. B., and Pert, A. (1985) Nicotinic binding in rat brain: autoradiographic comparison of [^{3}H]acetylcholine, [^{3}H]nicotine, and [^{125}I]α-bungarotoxin. *J. Neurosci.* **5,** 1307–1315
10. Dellisanti, C. D., Yao, Y., Stroud, J. C., Wang, Z.-Z., and Chen, L. (2007) Crystal structure of the extracellular domain of nAChR α1 bound to α-bungarotoxin at 1.94 A resolution. *Nat. Neurosci.* **10,** 953–962
11. Zouridakis, M., Giastas, P., Zarkadas, E., Chroni-Tzartou, D., Bregestovski, P., and Tzartos, S. J. (2014) Crystal structures of free and antagonist-bound states of human α9 nicotinic receptor extracellular domain. *Nat. Struct. Mol. Biol.* **21,** 976–980
12. Dubovskii, P. V., Konshina, A. G., and Efremov, R. G. (2014) Cobra cardiotoxins: membrane interactions and pharmacological potential. *Curr. Med. Chem.* **21,** 270–287
13. Antil-Delbeke, S., Gaillard, C., Tamiya, T., Corringer, P. J., Changeux, J. P., Servent, D., and Ménez, A. (2000) Molecular determinants by which a long chain toxin from snake venom interacts with the neuronal α7-nicotinic acetylcholine receptor. *J. Biol. Chem.* **275,** 29594–29601
14. Lyukmanova, E. N., Shenkarev, Z. O., Schulga, A. A., Ermolyuk, Y. S., Mordvintsev, D. Y., Utkin, Y. N., Shoulepko, M. A., Hogg, R. C., Bertrand, D., Dolgikh, D. A., Tsetlin, V. I., and Kirpichnikov, M. P. (2007) Bacterial expression, NMR, and electrophysiology analysis of chimeric short/long-chain α-neurotoxins acting on neuronal nicotinic receptors. *J. Biol. Chem.* **282,** 24784–24791
15. Mordvintsev, D. Y., Polyak, Y. L., Rodionov, D. I., Jakubik, J., Dolezal, V., Karlsson, E., Tsetlin, V. I., and Utkin, Y. N. (2009) Weak toxin WTX from *Naja kaouthia* cobra venom interacts with both nicotinic and muscarinic acetylcholine receptors. *FEBS J.* **276,** 5065–5075
16. Zhang, L., Zhang, Y., Jiang, D., Reid, P. F., Jiang, X., Qin, Z., and Tao, J. (2012) Alpha-cobratoxin inhibits T-type calcium currents through muscarinic M4 receptor and G*o*-protein $\beta\gamma$ subunits-dependent protein kinase A pathway in dorsal root ganglion neurons. *Neuropharmacology* **62,** 1062–1072
17. Gergalova, G., Lykhmus, O., Kalashnyk, O., Koval, L., Chernyshov, V., Kryukova, E., Tsetlin, V., Komisarenko, S., and Skok, M. (2012) Mitochondria express α7 nicotinic acetylcholine receptors to regulate Ca^{2+} accumulation and cytochrome c release: study on isolated mitochondria. *PLoS ONE* **7,** e31361
18. Shelukhina, I. V., Kryukova, E. V., Lips, K. S., Tsetlin, V. I., and Kummer, W. (2009) Presence of α7 nicotinic acetylcholine receptors on dorsal root ganglion neurons proved using knockout mice and selective α-neurotoxins in histochemistry. *J. Neurochem.* **109,** 1087–1095
19. Tsetlin, V., Shelukhina, I., Kryukova, E., Burbaeva, G., Starodubtseva, L., Skok, M., Volpina, O., and Utkin, Y. (2007) Detection of α7 nicotinic acetylcholine receptors with the aid of antibodies and toxins. *Life Sci.* **80,** 2202–2205
20. Bogdanov, Y., Michels, G., Armstrong-Gold, C., Haydon, P. G., Lindstrom, J., Pangalos, M., and Moss, S. J. (2006) Synaptic $GABA_A$ receptors are directly recruited from their extrasynaptic counterparts. *EMBO J.* **25,** 4381–4389
21. Joshi, S., Keith, K. J., Ilyas, A., and Kapur, J. (2013) $GABA_A$ receptor membrane insertion rates are specified by their subunit composition. *Mol. Cell. Neurosci.* **56,** 201–211
22. McCann, C. M., Bracamontes, J., Steinbach, J. H., and Sanes, J. R. (2006) The cholinergic antagonist α-bungarotoxin also binds and blocks a subset of GABA receptors. *Proc. Natl. Acad. Sci. U.S.A.* **103,** 5149–5154
23. Utkin, Y. N., Kukhtina, V. V., Kryukova, E. V., Chiodini, F., Bertrand, D., Methfessel, C., and Tsetlin, V. I. (2001) "Weak toxin" from *Naja kaouthia* is a nontoxic antagonist of α7 and muscle-type nicotinic acetylcholine receptors. *J. Biol. Chem.* **276,** 15810–15815
24. Osipov, A. V., Rucktooa, P., Kasheverov, I. E., Filkin, S. Y., Starkov, V. G., Andreeva, T. V., Sixma, T. K., Bertrand, D., Utkin, Y. N., and Tsetlin, V. I. (2012) Dimeric α-cobratoxin x-ray structure: localization of intermolecular disulfides and possible mode of binding to nicotinic acetylcholine receptors. *J. Biol. Chem.* **287,** 6725–6734
25. Tsetlin, V. I., Karlsson, E., Arseniev, A. S., Utkin, Y. N., Surin, A. M., Pashkov, V. S., Pluzhnikov, K. A., Ivanov, V. T., Bystrov, V. F., and Ovchinnikov, Y. A. (1979) EPR and fluorescence study of interaction of *Naja naja oxiana* neurotoxin II and its derivatives with acetylcholine receptor protein from *Torpedo marmorata*. *FEBS Lett.* **106,** 47–52
26. Starkov, V. G., Polyak, Y. L., Vulfius, E. A., Kryukova, E. V., Tsetlin, V. I., and Utkin, Y. N. (2009) New weak toxins from the cobra venom. *Russ. J. Bioorganic Chem.* **35,** 10–18
27. Grishin, E. V., Sukhikh, A. P., Slobodyan, L. N., Ovchinnikov YuA, and Sorokin, V. M. (1974) Amino acid sequence of neurotoxin I from *Naja naja oxiana* venom. *FEBS Lett.* **45,** 118–121
28. Maslennikov, I. V., Shenkarev, Z. O., Zhmak, M. N., Ivanov, V. T., Methfessel, C., Tsetlin, V. I., and Arseniev, A. S. (1999) NMR spatial structure of α-conotoxin ImI reveals a common scaffold in snail and snake toxins recognizing neuronal nicotinic acetylcholine receptors. *FEBS Lett.* **444,** 275–280
29. Mirheydari, P., Ramerstorfer, J., Varagic, Z., Scholze, P., Wimmer, L., Mihovilovic, M. M., Sieghart, W., and Ernst, M. (2014) Unexpected properties of δ-containing GABAA receptors in response to ligands interacting with the $\alpha+$ $\beta-$ site. *Neurochem. Res.* **39,** 1057–1067
30. Abràmoff, M. D., Magalhães, P. J., and Ram, S. J. (2004) Image processing with ImageJ. *Biophotonics Int.* **11,** 36–41
31. Guex, N., Peitsch, M. C., and Schwede, T. (2009) Automated comparative protein structure modeling with SWISS-MODEL and Swiss-PdbViewer: a historical perspective. *Electrophoresis* **30,** S162-S173
32. Pettersen, E. F., Goddard, T. D., Huang, C. C., Couch, G. S., Greenblatt, D. M., Meng, E. C., and Ferrin, T. E. (2004) UCSF Chimera–a visualization system for exploratory research and analysis. *J. Comput. Chem.* **25,** 1605–1612
33. Berendsen, H. J., van der Spoel, D., and van Drunen, R. (1995) GROMACS: A message-passing parallel molecular dynamics implementation. *Comput. Phys. Commun.* **91,** 43–56
34. Eastman, P., and Pande, V. (2015) OpenMM: a hardware-independent framework for molecular simulations. *Comput. Sci. Eng.* **12,** 34–39
35. Cornell, W. D., Cieplak, P., Bayly, C. I., Gould, I. R., Merz Jr., K. M., Ferguson, D. M., Spellmeyer, D. C., Fox, T., Caldwell, J. W., and Kollman, P. A. (1995) A second generation force field for the simulation of proteins, nucleic acids, and organic molecules. *J. Am. Chem. Soc.* **117,** 5179–5197
36. Humphrey, W., Dalke, A., and Schulten, K. (1996) VMD: visual molecular dynamics. *J. Mol. Graph.* **14,** 33–38
37. Bergmann, R., Kongsbak, K., Sørensen, P. L., Sander, T., and Balle, T. (2013) A unified model of the $GABA_A$ receptor comprising agonist and benzodiazepine binding sites. *PLoS ONE* **8,** e52323
38. Sigel, E., and Steinmann, M. E. (2012) Structure, function, and modulation of $GABA_A$ receptors. *J. Biol. Chem.* **287,** 40224–40231

39. Christian, C. A., Herbert, A. G., Holt, R. L., Peng, K., Sherwood, K. D., Pangratz-Fuehrer, S., Rudolph, U., and Huguenard, J. R. (2013) Endogenous positive allosteric modulation of $GABA_A$ receptors by diazepam binding inhibitor. *Neuron* **78,** 1063–1074
40. Alfonso, J., Le Magueresse, C., Zuccotti, A., Khodosevich, K., and Monyer, H. (2012) Diazepam binding inhibitor promotes progenitor proliferation in the postnatal SVZ by reducing GABA signaling. *Cell Stem Cell* **10,** 76–87
41. Bourne, Y., Talley, T. T., Hansen, S. B., Taylor, P., and Marchot, P. (2005) Crystal structure of a Cbtx-AChBP complex reveals essential interactions between snake α-neurotoxins and nicotinic receptors. *EMBO J.* **24,** 1512–1522
42. Utkin, Y. N., Krivoshein, A. V., Davydov, V. L., Kasheverov, I. E., Franke, P., Maslennikov, I. V., Arseniev, A. S., Hucho, F., Tsetlin, V. I. (1998) Labeling of *Torpedo californica* nicotinic acetylcholine receptor subunits by cobratoxin derivatives with photoactivatable groups of different chemical nature at Lys23. *Eur. J. Biochem.* **253,** 229–235
43. Hannan, S., Mortensen, M., and Smart, T. G. (2015) Snake neurotoxin α-bungarotoxin is an antagonist at native $GABA_A$ receptors. *Neuropharmacology* **93,** 28–40
44. Rosso, J.-P., Schwarz, J. R., Diaz-Bustamante, M., Céard, B., Gutiérrez, J. M., Kneussel, M., Pongs, O., Bosmans, F., and Bougis, P. E. (2015) MmTX1 and MmTX2 from coral snake venom potently modulate GABAA receptor activity. *Proc. Natl. Acad. Sci. U.S.A.* **112,** E891–E900
45. Sieghart, W. (2015) Allosteric modulation of GABAA receptors via multiple drug-binding sites. *Adv. Pharmacol.* **72,** 53–96
46. Hansen, S. B., Talley, T. T., Radic, Z., and Taylor, P. (2004) Structural and ligand recognition characteristics of an acetylcholine-binding protein from *Aplysia californica*. *J. Biol. Chem.* **279,** 24197–24202